

---

## Investigating Galaxy Clusters through $\gamma$ -ray Emission

---

Francesc Miniati

*Max-Planck-Institut für Astrophysik, Karl-Schwarzschild-Str. 1, 85740, Garching, Germany*

---

### Abstract

We address the role of  $\gamma$ -ray astronomy in the investigation of nonthermal processes in the large scale structure of the universe. Based on EGRET upper limits on nearby galaxy clusters (GCs) we constrain the acceleration efficiency of CR electrons at intergalactic shocks to  $\leq 1\%$  than the shock ram pressure. That implies a contribution to the cosmic  $\gamma$ -ray background from intergalactic shocks of order 25 % of the measured level. We model spatial and spectral properties of nonthermal  $\gamma$ -ray emission due to shock accelerated cosmic-rays (CRs) in GCs and *emphasize* the importance of imaging capability of upcoming  $\gamma$ -ray facilities for a correct interpretation of the observational results. GC observations at this photon energy will help us understand the origin of the radio emitting particles, the possible level of CR pressure and the strength of magnetic fields in intracluster environment and possibly will allow us detect the accretion shocks.

### 1. Introduction

Cosmic shocks emerge during structure formation in the universe, due to gravitationally driven supersonic gas infall onto collapsing objects. Astrophysical shocks are collisionless and capable of accelerating cosmic-rays (CRs) via first order Fermi mechanism [2]. CR electrons suffer severe energy losses dominated, in typical intra-cluster environment, by inverse Compton (IC) for energies above  $\sim 150$  MeV and Coulomb losses below that. Low energy, sub-relativistic CR protons also have short lifetimes due to Coulomb losses. However, for relativistic protons the dominant energy loss mechanism up to the energy threshold for photo-pair production is p-p inelastic collisions with a timescale longer than a Hubble time. Thus, once accelerated CR protons accumulate within large scale structures (LSSs) confined there by  $\mu\text{G}$  strong turbulent magnetic fields [22].

It is of interest to investigate CR acceleration at LSS shocks for several reasons. Firstly, GCs exhibit non-thermal radiation. This mainly consists of diffuse radio emission extending on Mpc scales. It is thought to be synchrotron

radiation but there is no consensus as to the origin of the emitting electrons. Also, excess of radiation with respect to thermal emission has been reported at hard X-ray [7] and, more controversially, extreme UV photon energies [10,4]. Secondly, if shocks acceleration operates efficiently, the proton component could bear a significant fraction of the total gas pressure, affecting the dynamics of cosmic structures [18]. Finally, CR electrons accelerated at inter-galactic shocks could contribute to the cosmic  $\gamma$ -ray background (CGB) [11]. This contribution addresses the role of  $\gamma$ -ray observations for investigating CR acceleration at LSS shocks. We describe the method in §2., the results in 3.-4. and conclude in §5.

## 2. Numerical Simulation

We perform numerical simulation that models simultaneously the formation of the LSS and the evolution of three CR species: namely *shock accelerated* protons and (primary) electrons and secondary  $e^\pm$  generated in p-p inelastic collisions of the simulated CR protons and the thermal gas. For the LSS we adopt a canonical, flat  $\Lambda$ CDM model with total mass density  $\Omega_m = 0.3$ , vacuum energy density  $\Omega_\Lambda = 0.7$ , Hubble constant  $H_0 = 67 \text{ km s}^{-1} \text{ Mpc}^{-1}$ , baryonic mass density,  $\Omega_b = 0.04$ , and spectral index and cluster normalization for initial density perturbations,  $n_s = 1$  and  $\sigma_8 = 0.9$  respectively (see ref. [14] for full details).

The CR dynamics, includes: injection at shocks, acceleration, energy losses and spatial transport. It is computed numerically through the code COSMOCR [13,14]. According to the adopted thermal leakage injection scheme, a fraction about  $10^{-4}$  of the protons crossing the shock is injected as CRs. For shocks with Mach number,  $M = 4 - 10$ , responsible for most of the heating of the intergalactic gas [14], this roughly corresponds to converting 30% of the shock ram pressure into CR proton pressure. Further, we assume that the ratio of accelerated primary CR electrons to protons at relativistic energies is given by a parameter  $R_{e/p} \sim 10^{-2}$  [12,1]. In accord to the test particle limit of diffusive shock acceleration theory [2], the accelerated particles are distributed in momentum as a power-law with slope  $q = 4/(1 - M^{-2})$ . All relevant loss mechanisms are accounted for [13,14]. We follow CR protons in the momentum range between 0.1 GeV/c and  $10^6$  GeV/c, and CR electrons and  $e^\pm$  between 15 MeV/c and 20 TeV/c.

## 3. Contribution to the Cosmic Gamma-ray Background

Fig. 1. (left) shows the contribution to the CGB from CRs accelerated at LSS shocks [14]. It is computed as

$$\varepsilon^2 J(\varepsilon) = \varepsilon \frac{c}{4\pi H_0} \int_0^{z_{max}} \frac{e^{-\tau_{\gamma\gamma}}}{[\Omega_m(1+z)^3 + \Omega_\Lambda]^{1/2}} \frac{j[\varepsilon(1+z), z]}{(1+z)^4} dz \quad (1)$$

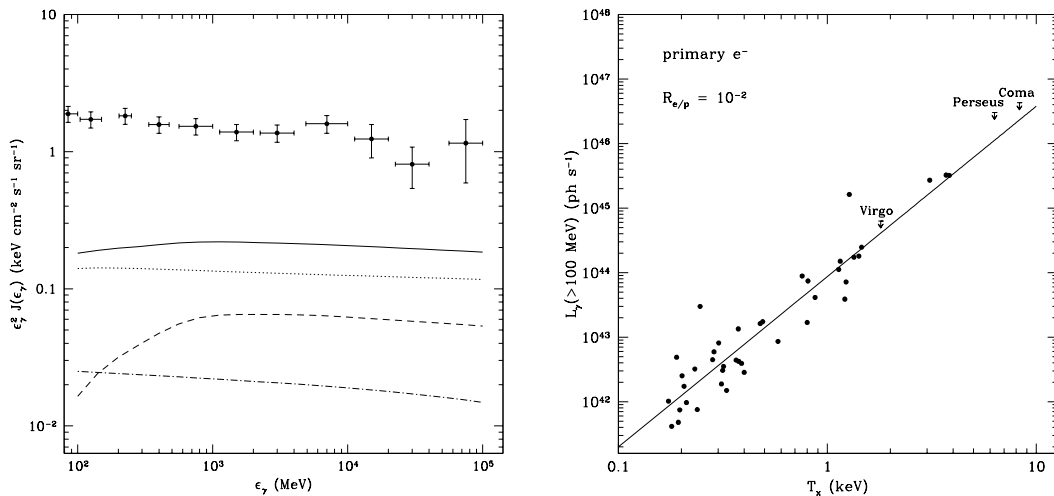


**Fig. 1.** *Left:*  $\gamma$ -ray background flux produced by cosmological CRs and EGRET data with their error-bars (solid dots) [21]. *Right:* The IC  $\gamma$ -ray photon luminosity above 100 MeV from individual clusters as a function of the cluster X-ray core temperature,  $T_x$ . EGRET experimental upper limits are from Reimer [19].

where  $\varepsilon$  is the photon energy,  $j(\varepsilon, z)$  is the computational-box-averaged spectral emissivity in units ‘photons  $\text{cm}^{-3} \text{s}^{-1}$ ’ at red-shift,  $z$ ,  $\tau_{\gamma\gamma}$  is an attenuation factor due to photo-pair creation,  $\gamma\gamma \rightarrow e^\pm$ ,  $c$  is the speed of light and  $z_{max}$  an upper limit of integration. EGRET observational data (solid dots) [21] are also shown for comparison. We consider the following emission processes: IC emission of CR electrons scattering off cosmic microwave background photons (dot line), decay of neutral pions ( $\pi^0 \rightarrow \gamma\gamma$ ) produced in p-p inelastic collisions (dash line) and IC emission from secondary  $e^\pm$  (dot-dash line). In fig. 1. the total flux (solid line) corresponds roughly to a constant value at the level of  $0.2 \text{ keV cm}^{-2} \text{ s}^{-1} \text{ sr}^{-1}$  throughout the spectrum. It is dominated by IC emission from primary electrons. Fractions of order 30% and 10 % are produced by  $\pi^0$ -decay and IC emission from secondary  $e^\pm$  respectively.

All three components produce the same flat spectrum, consistent with the observations. The result is a reflection of the fact that the CRs distributions were generated in strong shocks [14]. However, the computed flux is only  $\sim 15$  % of the observed CGB. It is difficult to imagine a higher contribution from  $\pi^0$ -decay and IC emission from  $e^\pm$ . In fact, if more CR protons were produced at shocks, CR-induced shock modifications would actually reduce the population of  $\gamma$ -ray emitting protons (and  $e^\pm$ ). On the other hand, the fraction,  $\eta$ , of shock ram pressure converted into CR electrons, can be constrained by comparing the

simulated clusters'  $\gamma$ -ray photon luminosity above 100 MeV to the upper limits set by the EGRET [20,19] for nearby GCs. This is done in fig. 1. (right panel). The simulation data are best-fit by the curve (solid line):

$$L_{\gamma}(> 100 \text{ MeV}) = 8.7 \times 10^{43} \left( \frac{\eta}{4 \times 10^{-3}} \right) \left( \frac{T_x}{\text{keV}} \right)^{2.6} \text{ ph s}^{-1}. \quad (2)$$

According to our calculations [14], the EGRET upper limits require that  $\eta \leq 0.8\%$ . This implies an upper limit on the computed  $\gamma$ -ray flux of about  $0.35 \text{ keV cm}^{-2} \text{ s}^{-1} \text{ sr}^{-1}$  or a fraction of order  $\sim 25\%$  of the CGB.

#### 4. Synthetic emission maps and spectrum for a Coma-like prototype

In this section we explore the spectral and spatial properties of  $\gamma$ -ray radiation between 10 keV and 10 TeV due to shock accelerated CRs in GCs. As non-thermal bremsstrahlung turns out unimportant [15], we consider the following emission processes:  $\pi^0$ -decay and IC emission from both primary CR electrons and secondary  $e^{\pm}$ . We first compute the emission spectrum for the largest virialized object in the computational box which has an X-ray core temperature  $T_x \simeq 4 \text{ keV}$ . The various emission components are then renormalized to the case of a Coma-like cluster. In particular, IC emission from electrons is rescaled according to equation 2. The total number of  $e^{\pm}$  is rescaled assuming that these particles are responsible for the synchrotron emission of Coma radio halo\*. For the purpose we took a radio flux at 1.4 GHz  $S_{1.4\text{GHz}} = 640 \text{ mJy}$  [5] and a two values for the volume average magnetic field  $\langle B \rangle$ , namely 1 and 3  $\mu\text{G}$  [9].

In the left quadrant of fig. 2. we present synthetic maps of the integrated photon flux above 100 keV (top panels) and 100 MeV (bottom panels). They show that the emission from  $\pi^0$ -decay (bottom left) and  $e^{\pm}$  (top left) is confined to the cluster core where it creates a diffuse halo which rapidly fades with distance from the center. In fact,  $e^{\pm}$  and  $\pi^0$  are produced at the highest rate in the densest regions where both the parent CR ions and target nuclei are most numerous. On the other hand, because of severe energy losses,  $\gamma$ -ray emitting primary electrons are only found in the vicinity of strong shocks where they are accelerated. The emission (right panels) is extended and with a rich morphology reflecting the complex “web” of accretion shocks surrounding GCs [17]. The corresponding synthetic spectra extracted from a core (top; with a  $0.5^\circ$  radius) and an outskirts region (bottom; a ring with inner and outer radii of  $0.5^\circ$  and  $1.5^\circ$  respectively) are shown in the central quadrant of fig. 2.. They shows that the emitted radiation in the outskirts region is strongly dominated by IC emission

---

\*This assumption is not necessary but it is assumed for simplicity

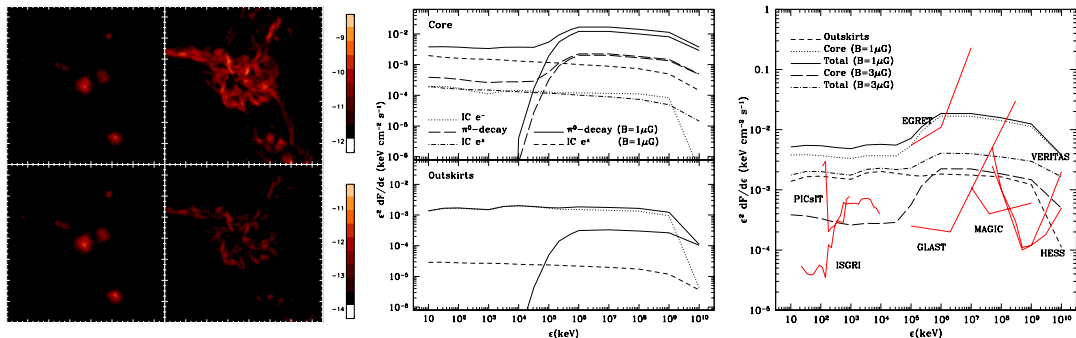


**Fig. 2.** *Left:* Synthetic map of the integrated photon flux in units “ph cm<sup>-2</sup> s<sup>-1</sup> arcmin<sup>-2</sup>”. Each panel measures 15  $h^{-1}$ Mpc on a side. *Center:* Synthetic spectra from 10 keV up to 10 TeV extracted from a core and an outskirts region. *Right:* Comparison of synthetic spectra with nominal sensitivity limits of future  $\gamma$ -ray observatories (thick-solid lines). Significance and observing time are respectively  $3\sigma$  and  $10^6$  s for INTEGRAL-IBIS imagers (ISGRI and PICsIT),  $5\sigma$  and one year of all sky survey for EGRET and GLAST and  $5\sigma$  and 50 hour exposure for the Cherenkov telescopes.

from primary primary  $e^-$ . Conversely in the core region  $\pi^0$ -decay (solid thin line) dominates at high photon energy ( $> 100$  MeV) (top panel). Below  $\sim 100$  MeV the relative contribution from primary and secondary  $e^\pm$  depends on the strength of the magnetic field. Finally, in the right quadrant the predicted radiation spectra in various spatial regions are compared to sensitivity limits<sup>†</sup> of planned  $\gamma$ -ray observatories.

## 5. Conclusions

Clusters observations at  $\gamma$ -ray energy will provide important information about GCs. First, the extended emission is produced at the location of accretion shocks which, unlike weak merging shocks, have yet to be observed *directly*. Thus, detection and imaging of IC emission from primary electrons would provide an opportunity for their direct observation. The flux about 100 keV together with radio measurements, will allow an estimate of the intracluster magnetic field. It is important, however, to separate out the contribution from the CR electrons accelerated at the outlining shocks. In fact, because the magnetic field strength is expected to drop at the cluster outskirts, these electrons likely generate only a weak radio emission. Nonetheless, they produce a strong IC flux which can easily

<sup>†</sup>These are for point sources and will be worse for extended sources considered here.

dominate the total soft  $\gamma$ -ray emission (cf. fig. 2.). Measuring the  $\gamma$ -ray flux at and above 100 MeV will allow us to confirm or rule out secondary  $e^\pm$  models for radio halos in GC [6,3,16] and to estimate the non-thermal CR pressure there [18]. In this perspective several authors estimated for nearby clusters the  $\gamma$ -ray flux from  $\pi^0$ -decay. However, radiation flux from IC emission can be comparable [15]. Therefore, for a correct interpretation of the measurements the contributions from these two components will need to be separated as outlined here.

Measuring the spectrum of IC  $\gamma$ -ray from primary CR electrons will also be instrumental for addressing their contribution to the CGB [11,14,8], the details of their acceleration mechanism and the physical conditions of the shocks.

## 6. Acknowledgments

This work is partially supported by the European Community under the contract HPRN-CT2000-00126 RG29185 (The Physics of the Intergalactic Medium). The computational work was carried out at the the Rechenzentrum in Garching.

1. Allen, G. E., Petre, R., & Gotthelf, E. V. 2001, *ApJ*, 558, 739
2. Blandford, R. D. & Eichler, D. 1987, *Phys. Rep.*, 154, 1
3. Blasi, P. & Colafrancesco, S. 1999, *Astropart. Phys.* , 12, 169
4. Bowyer, S., Berghoefter, T. W., & Korpela, E. 1999, *ApJ*, 526, 592
5. Deiss, B. M., Reich, W., Lesch, H., & Wielebinski, R. 1997, *A&A*, 321, 55
6. Dolag, K. & Enßlin, T. 2000, *A&A*, 362, 151
7. Fusco-Femiano, R., et al. 1999, *ApJ*, 513, L21
8. Keshet, U., et al. 2002, *ApJ*, in press (astro-ph/0202318)
9. Kim, K.-T., et al. 1990, *ApJ*, 355, 29
10. Lieu, R., et al. 1996, *Science* , 274, 1335
11. Loeb, A. & Waxman, E. 2000, *Nature*, 405, 156
12. Müller, D. & et al. 1995, in *Int. Cosmic Ray Conference*, Vol. 3, Rome, 13
13. Miniati, F. 2001, *Comp. Phys. Comm.* , 141, 17
14. Miniati, F. 2002, *MNRAS*, 337, 199
15. Miniati, F. 2002, *MNRAS*, submitted
16. Miniati, F., Jones, T. W., Kang, H., & Ryu, D. 2001, *ApJ*, 562, 233
17. Miniati, F., et al. 2000, *ApJ*, 542, 608
18. Miniati, F., Ryu, D., Kang, H., & Jones, T. W. 2001, *ApJ*, 559,
19. Reimer, O. 1999, in *ICRC*, Vol. 4, ed. D. Kieda, et al., Salt Lake City, 89
20. Sreekumar, et al. 1996, *ApJ*, 464, 628
21. Sreekumar, et al. 1998, *ApJ*, 494, 523
22. Völk, H. J., Aharonian, F. A., & Breitschwerdt, D. 1996, *Sp.Sci.Rev.*, 75, 279